Simple treatment of the enhancement of Raman scattering due to a two-dimensional array of metallic spheroids

Lan-Chan Chu
Institute of Electronics, National Chiao-Tung University, Hsinchu, Taiwan 300, Republic of China

Shou-yih Wang
Physics Department, National Tsing Hua University, Hsinchu, Taiwan 300, Republic of China
(Received 27 December 1983; revised manuscript received 6 July 1984)

A simple naive treatment of the enhancement of Raman scattering due to the presence of a two-dimensional array of metallic spheroids has been worked out as an extension of the existing particle-plasmon model. Calculated results, which are based on the r^{-3} term of dipolar fields, conform to the experiment. Comparisons and discussions show that this treatment, rather complete and accurate within the r^{-3} regime, provides the basic understanding of the physics of the spheroidal array experiment and also can serve to justify the existing single-spheroid approximations.

I. INTRODUCTION

It is well known that Raman scattering from some molecule adsorbed on a certain suitably roughened metal surface will be greatly enhanced.[1,2] This surface enhancement of Raman scattering (SERS) has drawn much attention of scientists for a number of years. An important advance in characterizing and investigating the SERS would be the experiments of Liao *et al.*,[3,4] using lithographically produced microspheroids of Ag, Au, and Al which are regularly arranged as a two-dimensional (2D) array. To explain the results, they employed the so-called particle-plasmon (PP) model[3,5,6] and simplified the treatment of the 2D array of spheroids by considering only a single isolated spheroid. The original PP model considers essentially the excitation of the molecule by the incident light and the local dipolar field of the spheroid as the first part which may be called the local-field enhancement. The second part, which may be called the Stokes field enhancement, is the emission of Raman field at Stokes frequency from the molecule and the single nearby spheroid owing to the necessity of satisfying the Maxwell boundary conditions at the spheroidal surface. The dielectric constant as a function of incident light frequency[7] and the morphology of the spheroid give the particle-plasmon resonance and the lightening-rod effect, respectively.[5] When the authors applied this PP model to the 2D array of spheroids with the spheroidal volume V and the depolarization factor A_j as adjustable parameters and with the introduction of radiation damping,[6] the resultant excitation profile, i.e., the total enhancement of Raman scattering versus incident frequency, is very satisfactory. Meanwhile, Barber *et al.* used an electrodynamical approach[8] to treat the SERS problem of the lithographically produced microspheroids and obtained desired results over the peak position and linewidth broadening for the SERS excitation profile. However, they still treated the 2D array as a simple isolated spheroid. To deal with the system as a truly 2D arrangement, Inoue and Ohtaka[9] recently studied a 2D array of spheres rather than spheroids and tried, as a partial purpose of their work, to explain the SERS problem. Their results appear rather unsatisfactory for the SERS and, as the authors claimed, the spheroidal array problem is still two complicated to treat at present.

The light scattering by a random distribution of 2D metal hemispheroids on an infinite perfect conducting flat surface was studied by Laor and Schatz.[10,11] They considered clusters and random distributions of the hemispheroids and used the long-wavelength approximation and dipole fields among the hemispheroids. This calculation obtains a new phenomenon of multiple plasmon resonances in an excitation profile and provided qualitatively similar results to that of experiment. However, their method, which was specially designed for random clusters, is not applicable to the calculation of the uniformly distributed spheroids in the arrangement of Liao *et al.*[3] Furthermore, the facts that their multiple resonance patterns depend too strongly on the number of hemispheroids and their calculated enhancement (10^2—10^3) for SERS are totally unsupported by experimental findings.

The aim of this work is to attack the apparently complicated 2D spheroidal array problem from a conceptually simple picture. The idea of this treatment is simply an extension of the formula of the PP model[3,6] with the single spheroid replaced by an array of spheroids. We feel it important to calculate the array problem beyond the single-spheroid approximation because the nearest-neighboring spheroids are located within the range of one wavelength of the incident light and their contributions and interference effects should not be entirely overlooked. Thus, although the present results of these single-spheroid treatments are satisfactory, we would like to work on the 2D problem and understand the underlying physics. Our simple formulation of the problem is given in Sec. II. Calculated results and comparisons with experiment and with some results calculated from Ref. 6 are shown in Sec. III. In Sec. IV we will discuss the results and draw conclusions.

II. FORMULATION OF THE CALCULATION

A. General description

Consider a system of a 2D array of identical spheroids each with the same effective aspect ratio c/d as shown in Fig. 1. The basic vectors $\vec{a},\vec{b}$ specify the spheroidal arrangement. Assume a plane wave $\vec{E}_i$ of light with frequency ω_0, unit polarization vector $\hat{e}_0$, and unit propagation vector $\hat{n}_0$ is incident upon the spheroidal array. As most of the authors have done in treating the SERS problems we restrict the consideration to only the dipolar oscillation of each spheroid with essentially only the near-field dependence r^{-3}, where r is the distance measured from the dipole to the molecule. The molecule which gives the Raman scattering is assumed sitting on the tip of the spheroid at origin, i.e., with coordinates $\vec{r}_l=(0,0,-c)$. The molecule is considered as a classical point dipole and assumed for simplicity to oscillate with its electric dipole moment p_m only in z direction, i.e.,

$$\vec{p}_m=p_m\hat{z}\ , \tag{1}$$

where $\hat{z}$ is the unit vector along the Z axis. Now we have two situations to compare:[12] one with the spheroidal array arranged as Fig. 1 and the other without the array. When the array exists we have the molecular dipole $\vec{p}_m$, the primary electric field $\vec{E}_p$, and the Raman shifted or Stokes field $\vec{E}_R$:

$$\vec{p}_m=\vec{\vec{\alpha}}\cdot\vec{E}_p(\vec{\gamma}_l,\omega_0)\ , \tag{2}$$

$$\vec{E}_p(\vec{\gamma}_l,\omega_0)=\vec{E}_i(\vec{\gamma}_l,\omega_0)+\vec{E}_{ar}(\vec{\gamma}_l,\omega_0)\ , \tag{3}$$

$$\vec{E}_R(\vec{r},\omega)=\vec{E}_{di}(\vec{r},\omega)+\vec{E}_{sc}(\vec{r},\omega)\ , \tag{4}$$

where $\vec{\vec{\alpha}}$ is the molecular polarizability tensor. $\vec{E}_{ar}$, $\vec{E}_{di}$, and $\vec{E}_{sc}$ are the fields arising from the spheroidal array, the molecular dipole field, and the scattered field again due to array of spheroids, respectively. We note that the Stokes fields $\vec{E}_R$, $\vec{E}_{di}$, and $\vec{E}_{sc}$ are evaluated at observation point $\vec{r}$ and with Stokes frequency ω. When the array is absent, we have a sole molecule at $\vec{r}_l$ with its dipole moment $\vec{p}\,'_m$ and Stokes field $\vec{E}\,'_R$, respectively, given by

$$\vec{p}\,'_m=\vec{\vec{\alpha}}\cdot\vec{E}_i(\vec{\gamma}_l,\omega_0)\ , \tag{5}$$

$$\vec{E}\,'_R=\vec{E}\,'_{di}(\vec{r},\omega)\ . \tag{6}$$

Here, we use the same polarizability tensor $\vec{\vec{\alpha}}$ and exclude any chemical effect due to the nearby spheroids. $\vec{E}\,'_{di}$ is the molecular dipole field due to $\vec{p}\,'_m$. Furthermore, we assume for simplicity $\vec{\vec{\alpha}}$ as a scalar α_m and, with Eq. (1), we have

$$p_m=\alpha_m E_{pz}(\vec{\gamma}_l,\omega_0)\ , \tag{7}$$

where E_{pz} is the z component of $\vec{E}_p$. The SERS enhancement factor f due to the presence of spheroids is then

$$f=\left|\frac{\vec{E}_R(\vec{r},\omega)}{\vec{E}\,'_R(\vec{r},\omega)}\right|^2$$

$$=\frac{|\vec{E}_R(\vec{r},\omega)|^2}{|\vec{E}_{di}(\vec{r},\omega)|^2}\frac{|\vec{E}_{di}(\vec{r},\omega)|^2}{|\vec{E}\,'_{di}(\vec{r},\omega)|^2}=\frac{|\vec{E}_R(\vec{r},\omega)|^2}{|\vec{E}_{di}(\vec{r},\omega)|}\left|\frac{\vec{p}_m}{\vec{p}\,'_m}\right|^2$$

$$=\left|\frac{\vec{E}_R(\vec{r},\omega)}{\vec{E}_{di}(\vec{r},\omega)}\right|^2\left|\frac{E_{pz}(\vec{\gamma}_l,\omega_0)}{E_{iz}(\vec{\gamma}_l,\omega_0)}\right|^2$$

$$\equiv f_2 f_1\ , \tag{8}$$

where E_{iz} is the z component of $\vec{E}_i$ and Eq. (7) has been used. The local-field enhancement f_1 of incident-light frequency ω_0 and the Stokes field enhancement f_2 of Stokes frequency ω are defined, respectively, by

$$f_1=\frac{|E_{pz}(\vec{\gamma}_l,\omega_0)|^2}{|E_{iz}(\vec{\gamma}_l,\omega_0)|^2} \tag{9}$$

and

$$f_2=\frac{|\vec{E}_R(\vec{r},\omega)|^2}{|\vec{E}_{di}(\vec{r},\omega)|^2} \tag{10}$$

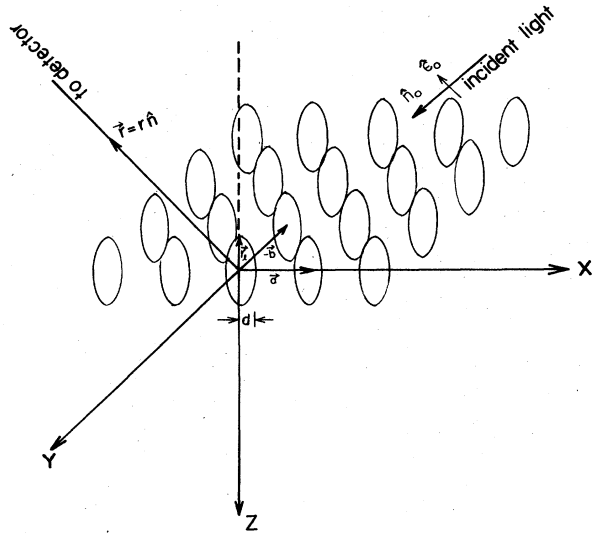

FIG. 1. Arrangement of the 2D array of spheroids.

B. Polarizability of a single spheroid

Assuming the ratio of spheroid volume V to the cube of incident-light wavelength is small, i.e., $V/\lambda^2\ll 1$, which is reasonable for the experimental data,[3,4] we have the electrical field[13] inside the spheroid of the array:

$$E_j=\frac{1}{1+(\epsilon-1)A_j}(\vec{E}_i)_j,\quad j=x,y,z \tag{11}$$

$$A_x = A_y = \frac{m}{2(m^2-1)}\left[m - \frac{1}{2(m^2-1)^{1/2}} \times \ln\left[\frac{m+(m^2-1)^{1/2}}{m-(m^2-1)^{1/2}}\right]\right], \quad (12)$$

$$A_z = \frac{1}{m^2-1}\left[\frac{m}{2(m^2-1)^{1/2}} \ln\left[\frac{m+(m^2-1)^{1/2}}{m-(m^2-1)^{1/2}}\right] - 1\right], \quad (13)$$

where $m = c/d$; c, d, A_x, A_y, A_z (Ref. 14), and ϵ (Ref. 7) are the semimajor and semiminor axes, depolarization factors along X, Y, Z axes, and the dielectric constant of the spheroid, respectively. The polarization of the spheroid P_j is

$$P_j = \frac{\epsilon - 1}{4\pi} E_j \, . \quad (14)$$

The electric dipole moment of the spheroid, p_j, is the product of its volume and the polarization P_j, viz.,

$$p_j = -\tfrac{1}{3} c d^2 \frac{1-\epsilon}{1-(1-\epsilon)A_j} (\vec{E}_i)_j \, , \quad (15)$$

which yields the diagonal polarizability tensor of the spheroid μ_j:

$$\mu_j = -\tfrac{1}{3} c d^2 \frac{1-\epsilon}{1-(1-\epsilon)A_j} \, . \quad (16)$$

C. Dipole fields, radiation damping, and the weighting function

A point dipole of moment $\vec{p}\,'$ oscillating with frequency ω' will give rise to a near field at $\vec{r}$ (Ref. 13),

$$\vec{E}_{ne} = [3\hat{n}(\hat{n}\cdot\vec{p}\,') - \vec{p}\,'] \frac{e^{ik_d r}}{r^3} \, , \quad (17)$$

where $\hat{n}$ is the unit vector along $\vec{r}$, $k_d = \omega'/c_0$, and c_0 is the speed of light in that medium. This is essentially the only dipolar field which is of concern. The far field of the dipole, E_{far},

$$\vec{E}_{\text{far}} = k_d^2 (\hat{n} \times \vec{p}\,') \times \hat{n} \frac{e^{ik_d r}}{r} \, , \quad (18)$$

is normally the source for the Stokes signal at the detector region. However, as far as the enhancement factor f is concerned, the r^{-1} dependence would be canceled out in the calculation of f_2 of Eq. (10).

Radiation damping may be regarded as a necessary process for a finite-size oscillating dipole.[6,15] Meier and Wokaun expanded the Mie dipole coefficient and tried to derive the radiation damping term.[16] Since the spheroid is treated as a point dipole of dipole moment p_j sitting at the center of the spheroid the finite-size radiation effect has to be taken into consideration, which simply requires the replacement of the depolarization factor A_j by the effective depolarization factor:[6]

$$A_j^{\text{eff}} = A_j + i\,4\pi^2 V/3\lambda^3 \, , \quad (19)$$

where λ and V are, respectively, the incident-light wavelength and spheroidal volume.

There is another important deficiency in assuming the point dipole sitting at the center of the spheroid.[2,3] Clearly, if the dipole is imagined to lie near the tip of the spheroid instead of sitting at the center, the near field of the dipole acting on the molecule would be much stronger. Thus, the correct treatment[6] should stem from the Maxwell's equations and the boundary conditions at the spheroidal surface, which is mainly the continuity at the boundary of the normal component of displacement current vector $\vec{D}$. Since we want to treat an array of many spheroids, the precise matching of boundary condition of all spheroids would be too tedious. Instead, we replace each spheroid by a point dipole at its center and then introduce a frequency-dependent weighting function $W_{mn}(\omega')$ to correct the deficiency. The integers m,n of $W_{mn}(\omega')$ denote the location $(m\vec{a}+n\vec{b})$ of the spheroid in the 2D array. Conditions on $W_{mn}(\omega')$ would be

$$W_{mn}(\omega') \to \begin{cases} 1, & m,n \gg 1 \quad (20) \\ \frac{3}{2}\left[\frac{c}{d}\right]^2 \left[1 - \left[A_z + i\tfrac{4}{3}\pi^2 \frac{V}{\lambda^3}\right]\right], & m = n = 0 \quad (21) \end{cases}$$

where the weighting function for the spheroid at origin

$$\tfrac{3}{2}(c/d)^2 \left[1 - \left[A_z + i\tfrac{4}{3}\pi^2 \frac{V}{\lambda^3}\right]\right]$$

is approximately the factor distinguished between the enhancement due to a point dipole at center[3] and that due to matching of the correct Maxwell's boundary conditions.[6] The condition (20) means that, at far distances from the spheroid under consideration, the dipole location at the center or at the boundary of the spheroid should give no difference. We take the distance variation of the weighting function as that of dipolar near field. Thus, a convenient form of $W_{mn}(\omega')$ is taken:

$$W_{mn}(\omega') = 1 + \left\{\frac{3}{2}\left[\frac{c}{d}\right]^2 \left[1 - \left[A_z + i\tfrac{4}{3}\pi^2 \frac{V}{\lambda^3}\right]\right] - 1\right\} c^3 \Big/ (m^2a^2 + n^2b^2 + c^2)^{3/2} \, . \quad (22)$$

D. f_1 and f_2

Taking all these into consideration, we have, for the primary field of Eq. (3),

$$\vec{E}_i=\hat{\epsilon}_0 E_0 e^{ik_0\hat{n}_0\cdot\vec{r}_l}, \tag{23}$$

$$\vec{E}_{ar}(\vec{r}_l,\omega_0)=\sum_{m,n} W_{mn}(\omega_0)[\,3\vec{T}'_{mn}(\vec{T}'_{mn}\cdot\vec{p}_{mn})-\vec{p}_{mn}|\vec{T}'_{mn}|^2]\frac{e^{ik_0|\vec{T}'_{mn}|}}{|\vec{T}'_{mn}|^5},$$

where

$$k_0=\frac{\omega_0}{c_0}, \tag{24}$$

$$\vec{T}'_{mn}=\vec{T}_{mn}+\vec{r}_l, \tag{25}$$

$$\vec{T}'_{mn}=m\vec{a}+n\vec{b}, \tag{26}$$

$$\vec{p}_{mn}=\vec{p}e^{ik_0\hat{n}_0\cdot\vec{T}_{mn}}. \tag{27}$$

With the spheroid dipole moment $\vec{p}$ induced by the incident light given by Eq. (15), we consider only a p-polarized wave which produces z-component local field at $(0,0,-c)$. Substitution of these into Eq. (9) yields the local-field enhancement

$$f_1=\left|1+\frac{\vec{E}_{ar}\cdot\hat{z}}{\hat{\epsilon}_0\cdot\hat{z}E_0e^{ik_0\hat{n}_0\cdot\vec{r}_l}}\right|^2, \tag{28}$$

where

$$\hat{n}_0=(\sin\theta\cos\phi,\sin\theta\sin\phi,\cos\theta), \tag{29}$$

$$\hat{\epsilon}_0=(\cos\theta\cos\phi,\cos\theta\sin\phi,-\sin\theta). \tag{30}$$

To calculate f_2, we first obtain the secondary field $\vec{E}_{sc}$ of Eq. (4). The molecule at $\vec{r}_l$ after being excited by the primary local field $\vec{E}_p$ of Eq. (3) oscillates and emits fields $\vec{E}_{mn}$, again corrected with the weighting function $W_{mn}(\omega)$, to each lattice point (m,n) of the 2D array. The $\vec{E}_{mn}$ polarizes in turn each metallic spheroid of polarizability u_j of Eq. (16) at Stokes frequency ω. The resultant spheroid dipole moments $\vec{D}_{mn}$ at all locations (m,n) give rise the scattered fields $\vec{E}_{sc}$ and contribute to the final Raman signal. Explicitly,

$$\vec{E}_{mn}=W_{mn}(\omega)p_m[3\vec{R}_{mn}(\vec{R}_{mn}\cdot\hat{z})-\hat{z}|\vec{R}_{mn}|^2]\frac{e^{ik|\vec{R}_{mn}|}}{|\vec{R}_{mn}|^5}, \tag{31}$$

where

$$\vec{R}_{mn}=\vec{T}_{mn}-\vec{r}_l, \tag{32}$$

$$k=\omega/c_0. \tag{33}$$

The spheroidal dipole moment $\vec{D}_{mn}$ induced by $\vec{E}_{mn}$ should take the form

$$\vec{D}_{mn}=p_m W_{mn}(\omega)\frac{e^{ik|\vec{R}_{mn}|}}{|R_{mn}|^5}[3cu_x(\omega)(ma\hat{x}+nb\hat{y})+(3c^2-|\vec{R}_{mn}|^2)u_z(\omega)\hat{z}]$$

$$\equiv p_m\vec{D}'_{mn}, \tag{34}$$

where $\hat{x},\hat{y}$ are the unit vectors along X,Y axes. The Stokes field enhancement f_2, thus, becomes

$$f_2=\left|(\hat{n}\times\hat{z})\times\hat{n}e^{-ik\hat{n}\cdot\vec{r}_l}+\sum_{m,n}(\hat{N}\times\vec{D}'_{mn})\times\hat{n}e^{-ik\hat{n}\cdot\vec{T}_{mn}}\right|^2 \times[\,|(\hat{n}\times\hat{z})\times\hat{z}|^2]^{-1} \tag{35}$$

in which

$$\hat{n}=(\sin\theta_o\cos\phi_o,\sin\theta_o\sin\phi_o,\cos\theta_o) \tag{36}$$

denotes the direction of the observed Stokes signal at the detector. The overall enhanced factor is obtained from the product of f_1 and f_2 as given in Eq. (8).

III. RESULTS AND COMPARISONS

We take $a=b=3000$ Å to match the experimental conditions and set the spherical angles for the direction of the incident light $\theta=60°,\phi=0°$, and those of the observer at the detector $\theta_o=150°,\phi_o=180°$. In Fig. 2 we show our calculated results for Ag with the spheroidal radius $d=258$ Å and aspect ratio 4.0/1.0. The local-field enhancement f_1 and the Stokes field enhancement f_2 are plotted for comparison. They are approximately coincident for incident-photon energies around the peak. This is similar to that of the single-spheroid calculation in

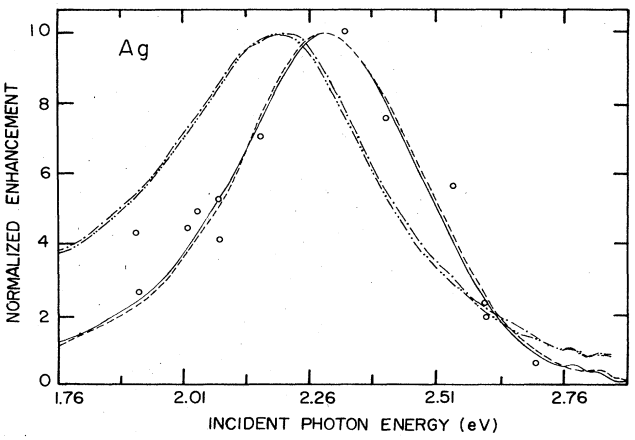

FIG. 2. Normalized enhancement for Ag versus incident photon energies: $a=3000$ Å, $c=1034$ Å, $d=258$ Å, $\phi=0°$, $\phi_o=180°$, $\theta=60°$, $\theta_o=150°$. Solid line for the total enhancement f; dashed line obtained from a formula of Ref. 6; circles for the experimental data; dashed-dotted line for local-field enhancement f_1; and dashed–double-dotted line for Stokes field enhancement f_2.

which these functions are identical.[3,6] The solid line is the calculated total SERS enhancement factor f of Eq. (8) which shows excellent agreement with the experimental data denoted by circles. The shift in the peak position of f from the peak positions of f_1 and f_2 results from the difference between the laser frequency of f_1 and the Stokes frequency of f_2. Another comparison is made with the results (dashed lines) calculated from a formula given by Liao *et al.*[4,6] which assumes a single-spheroid instead of a single-spheroid array. As seen clearly in the figure, the peak value of f due to their result is 2.56×10^6 and that of our result is 2.74×10^6. This slight discrepancy between calculated results of the single-spheroid approximation and that of our more realistic model of arrayed spheroids can be traced out as due to mainly the relatively short-ranged r^{-3} dipolar field used. To be more specific to this point, one may estimate for a typical case, the contribution from the first nearest spheroids to the z component of the field $\vec{E}_p$ at the molecule site $(0,0,-c)$ using Eq. (23). The ratio of this contribution to that from the central spheroid $(m=0,n=0)$ is ~0.01 due to the rapidly diminishing dipolar-field dependence r^{-3} alone. The phase interference arising from these four nearest neighbors further reduces the field at $(0,0,-c)$ by a factor of ~0.1. Thus the field contribution due to the first nearest neighbors is totally about 0.001 smaller than that from the single central spheroid. Consequently, although an infinite number of spheroids of the array could contribute to the field, the enhancement factor, which is roughly proportional to the fourth power of field strength, can increase only slightly. For the long-range dipolar-field terms r^{-2} and r^{-1}, the contribution may be substantial. However, that problem is beyond the scope of the r^{-3} dipolar field of this paper. It is being done and will be reported elsewhere. Figure 3 gives the plots for Au with spheroidal radius $d=270$ Å, and aspect ratio 4.1/1.0.

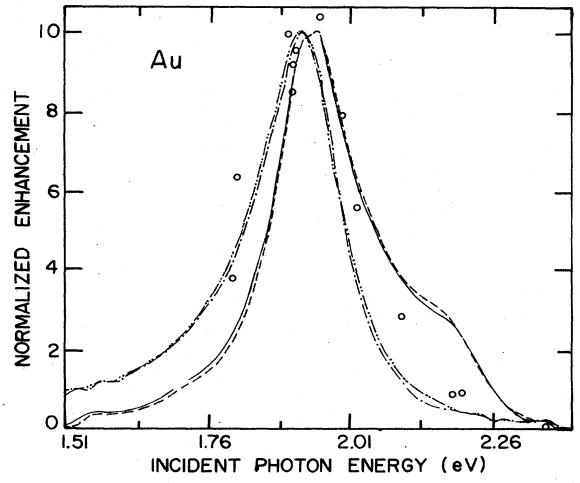

FIG. 3. Normalized enhancement for Au versus incident photon energies: $a=3000$ Å, $c=1107$ Å, $d=270$ Å, $\phi=0°$, $\phi_o=180°$, $\theta=60°$, $\theta_o=150°$. Solid line for the total enhancement f; dashed line obtained from a formula of Ref. 6; circles for the experimental data; dashed-dotted line for local-field enhancement f_1; and dashed—double-dotted line for Stokes field enhancement f_2.

Notations are similar to those of Fig. 2 for Ag. The main difference between Au and Ag is that the imaginary part of dielectric constant of the former[7] is remarkably larger than that of the latter.[7] This should account for all the differences between Figs. 2 and 3. In this figure we note the relatively smaller shift in the peak position of the total enhancement from that of f_1 or f_2. The occurrence of a shoulder at photon energy ~2.19 eV would arise from the feature of the dielectric constants and the frequency difference between the laser frequency of f_1 and the Stokes frequency of f_2. The dashed line, which is calculated[4] from the single-spheroid model as in Fig. 2, is still almost as good as ours. In Fig. 4, we present another result for Au with spheroidal radius $d=269$ Å and aspect ratio 3.8/1.0, the same set of values used in Ref. 4. Our calculated curve (solid line) is almost coincident with that of Ref. 4 except in the region of photon energies ~2.12 eV. Clearly, the experimental data are not as well substantiated by the calculated curves as those shown in Fig. 3. The only difference between these two figures lies in the data of d and c, or more clearly the spheroidal radius d and the aspect ratio (c/d). Comparison between these two figures shows that the aspect ratio 4.10/1.0 is more appropriate than 3.8/1.0 for Au, because the semiminor axis d used in the two figures differs only slightly. At this point, we like to make a few remarks: (1) The aspect ratio, which plays a very important role in these SERS problems, should have some distribution around its mean value. We have investigated the effects due to the aspect ratio distribution and have reported them elsewhere.[17] (2) The radius or the semiminor axis d (270 Å) for Au is much smaller than the radius of the base of SiO_2 core (500 Å) as given in Fig. 1 of Ref. 3, which has been used in Fig. 3 of Ref. 8. Calculations with such a larger radius (500 Å) based either on a single-spheroid model[8] or on this spheroid-array model all indicate that the very broad linewidth, much smaller magnitude, and the peak position of the enhancement factor simply cannot be verified by

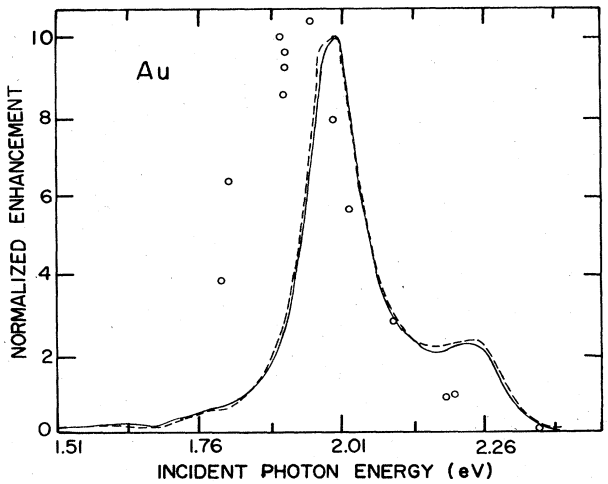

FIG. 4. Normalized enhancement for Au versus incident photon energies: $a=3000$ Å, $c=1020$ Å, $d=269$ Å, $\phi=0°$, $\phi_o=180°$, $\theta=60°$, $\theta_o=150°$. Solid line for the total enhancement f; dashed line obtained from a formula of Ref. 6.

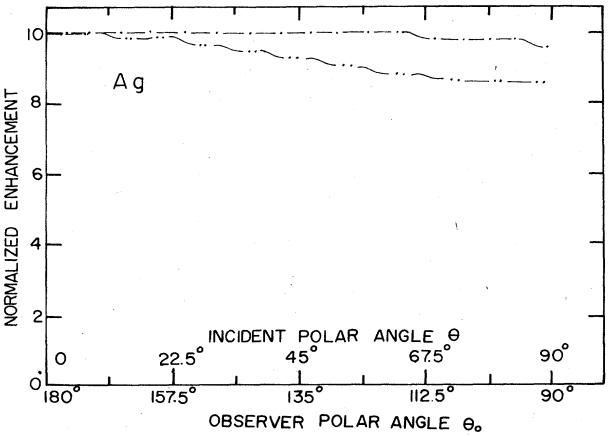

FIG. 5. Normalized enhancement for Ag versus incident and observer polar angles θ and θ_o, respectively: $a=3000$ Å, $c=1034$ Å, $d=258$ Å, $\phi=0°$, $\phi_o=180°$, photon energy 2.55 eV. Dash-dotted line for local-field enhancement f_1 with fixed $\theta_o=150°$ and variable θ from 0° to 90°; dashed—double-dotted line for Stokes field enhancement f_2 with fixed $\theta=30°$ and variable θ_o from 90° to 180°.

the experimental results. We are, then, led to conclude that the effective or equivalent radius of the actual spheroid under consideration must be much less than the nominal value 500 Å. (3) The local radius of curvature near the tip of a spheroid, which could be largely distorted in shape and size from that of the geometric spheroid, would be the truly effective radius in producing the SERS effect. Thus, both the semiminor axis d and the aspect ratio c/d should be regarded as the effective values rather than their formal numbers.

The angular dependence of the total enhancement on the orientation of the incident light and that of the Stokes light at the detector is shown in Fig. 5 (for Ag at fixed photon energy 2.55 eV) and Fig. 6 (for Au at fixed photon energy 2.11 eV). For the upper curve (denoted by the dash-dotted line) of both figures, the orientation of the incident light, specified by the spherical angles (θ,ϕ), is taken to vary θ from 0° to 90° while the orientation (θ_o,ϕ_o) of the Stokes light at the detector is kept fixed at $\theta_o=150°$. Since the system of the spheroid array has azimuthal symmetry, we may arbitrarily set $\phi=0°$, $\phi_o=180°$. For the lower curves (denoted by the dash-double-dotted line) the orientation of the incident light is kept fixed at $\theta=30°$ while the orientation θ_o is taken to vary from 90° to 180°. The general feature of the enhancement f curve appears to be flat over nearly the whole available range of polar angles θ and θ_o for both Ag and Au. This weak dependence on angles is in accord with the experimental observation.[3]

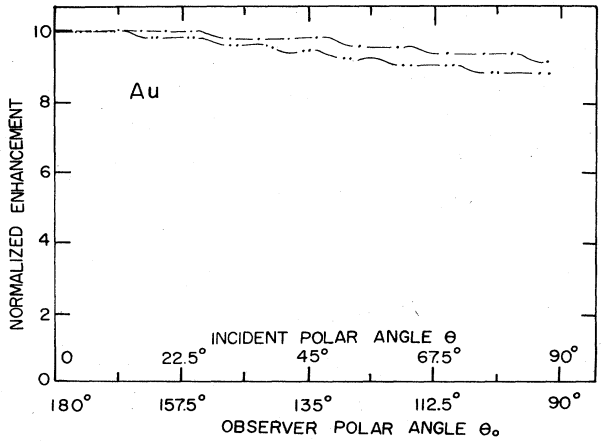

FIG. 6. Normalized enhancement for Au versus incident and observer polar angles θ and θ_o, respectively: $a=3000$ Å, $c=1107$ Å, $d=270$ Å, $\phi=0°$, $\phi_o=180°$, photon energy 2.11 eV. Dash-dotted-line for local-field enhancement f_1 with fixed $\theta_o=150°$ and variable θ from 0° to 90°; dashed—double-dotted line for Stokes field enhancement f_2 with fixed $\theta=30°$ and variable θ_o from 90° to 180°.

IV. DISCUSSIONS AND CONCLUSIONS

This simple calculation has neglected the mutual interactions among the spheroids as well as the multireflections among these spheroids. The mutual interaction (referring to the change in the dipole moment due to the presence of a neighboring dipole) is basically a dipole-dipole interaction and therefore should behave like r^{-6} with the spatial separation r between two neighboring spheroids. As stated in Sec. III the short-range dipolar field (r^{-3}) contributes only ~ 0.01 from a neighboring spheroid to the central one. The dipole-dipole contribution ($\sim r^{-6}$) from a nearest-neighbor spheroid would accordingly affect the field at the tip of the central spheroid by a factor ~ 0.0001. This should give a negligible effect to the overall enhancement f, which is roughly proportional to the fourth power of the field. As to the multiple reflections among the arrayed spheroids we note that each reflection by a certain spheroid would reduce the field magnitude at least by ~ 0.01 due to the short-range r^{-3} dipolar field. For example, assume an incident light from the central spheroid to a nearest neighbor is reflected back to the central one. The contribution in the electric field at the central spheroid would be at most ~ 0.0001 of the original field magnitude. Consequently, the neglect of the dipole-dipole mutual interaction and multiple reflections is justifiable in our simple calculation.

Another thing we must mention is the phase retardation. It accounts for the effect due to the phase change within a wavelength of incident light that acts on an object of size comparable to the wavelength. Within the particle-plasmon model which was originally an electrostatic calculation, Gersten and Nitzan,[5] Laor and Schatz,[10] and Liao *et al.*[3,6] have not given such an account. Only in the electrodynamical calculation given by Barbar *et al.*,[8] which treated a single-spheroid instead of 2D spheroidal array, have the effects of phase retardation been explicitly disclosed. It produces a reduction in the magnitude of SERS enhancement, a relatively large broadening of linewidth, a shift of peak position of enhancement toward longer wavelength, and an additional multipole peak in the excitation profile.[8] This calculation was for a spheroid of radius of 500 Å, of which the results are not in agreement with experiment.[3] For a much smaller spheroid of radius 258 Å for Ag and 270 Å for Au (less than 10% of the incident-light wavelength), such

as the cases of this paper, the electrodynamic phase retardation effects should be much less pronounced. Our calculation is a corrected long-wavelength approximation of an electrodynamical approach which takes into consideration the effect of phases as given in Eq. (23) and Eq. (34) but not of the phase retardation (i.e., long-wavelength approximation) from different locations of the spheroid, nor the full effects of r^{-1} and r^{-2} dipolar fields. Yet we add the radiation damping as a correction term following the works of Wokaun *et al.*[6] and Meier and Wokaun.[16] According to the latter reference of a single-sphere calculation, the phase retardation effect is manifested mainly as the dynamical depolarization and the radiation damping. However, since the effect of dynamical depolarization is important only for very small particle sizes,[16] the radiation damping effect is dominant in our cases. So we believe our treatment has included the main feature of a complete electrodynamic treatment ever found for the 2D regular array of metal spheroids.

In conclusion we have given, for the first time, a method of calculation for a 2D array of spheroids. the idea of the method appears simple, naive, and elegant. The calculated results, although only slightly improving those numerical results of Liao *et al.*[3,4] which have already conformed well to experiment, can serve as well to justify the validity of the single-spheroid approximations and provide the basic understanding of the underlying physics of the spheroidal array problem.

ACKNOWLEDGMENT

This work was financially sponsored by the National Science Council of the Republic of China.

[1]M. Fleischmann, P. J. Hendra, and A. J. Mcquillan, Chem. Phys. Lett. **26**, 163 (1974).
[2]R. K. Chang and T. E. Furtak, *Surface Enhanced Raman Scattering* (Plenum, New York, 1982).
[3]P. F. Liao, J. G. Bergman, D. S. Chemla, A. Wokaun, J. Melngailis, A. M. Hawryluk, and N. P. Economou, Chem. Phys. Lett. **82**, 355 (1981).
[4]P. F. Liao and M. B. Stern, Opt. Lett. **7**, 483 (1982).
[5]J. Gersten and A. Nitzan, J. Chem. Phys. **73**, 3023 (1980).
[6]A. Wokaun, J. P. Gordon, and P. F. Liao, Phys. Rev. Lett. **48**, 957 (1982).
[7]P. B. Johnson and R. W. Christy, Phys. Rev. B **6**, 4370 (1972).
[8]P. W. Barber, R. K. Chang, and H. Massoudi, Phys. Rev. Lett. **50**, 997 (1983).
[9]Masaahiro Inoue and Kazuo Ohtaka, J. Phys. Soc. Jpn. **52**, 1457 (1983).
[10]U. Laor and G. C. Schatz, Chem. Phys. Lett. **82**, 566 (1981).
[11]U. Laor and G. C. Schatz, J. Chem. Phys. **76**, 2888 (1982).
[12]M. Kerker, D.-S. Wang, and H. Chew, Appl. Opt. **19**, 4159 (1980).
[13]C. J. F. Boettcher, *Theory of Electric Polarization,* 2nd ed. (Elsevier, New York, 1973), Chap. 2.
[14]J. A. Osborn, Phys. Rev. **67**, 351 (1945).
[15]J. D. Jackson, *Classical Electrodynamics* (Wiley, New York, 1975), pp. 395 and 783.
[16]M. Meier and A. Wokaun, Opt. Lett. **8**, 581 (1983).
[17]L. C. Chu and S. Y. Wang, J. Appl. Phys. **55**, 2776 (1984).